ISSN 1807-1929
Revista Brasileira de Engenharia Agrícola e Ambiental
Brazilian Journal of Agricultural and Environmental Engineering
v.26, n.4, p.283-291, 2022
Campina Grande, PB – http://www.agriambi.com.br – http://www.scielo.br/rbeaa

DOI: http://dx.doi.org/10.1590/1807-1929/agriambi.v26n4p283-291

Automation of monitoring of drying parameters in hybrid solar-electric dryer for agricultural products[1]

Automação do monitoramento dos parâmetros de secagem em secador híbrido solar-elétrico para produtos agrícolas

Juliana L. Paes[2*], Vinícius de A. Ramos[2], Marcus V. M. de Oliveira[2], Marinaldo F. Pinto[2], Thais A. de P. Lovisi[2] & Wagner D. de Souza[2]

[1] Research developed at Rio de Janeiro, RJ, Brazil
[2] Universidade Federal Rural do Rio de Janeiro/Instituto de Tecnologia/Departamento de Engenharia, Seropédica, RJ, Brazil

HIGHLIGHTS:
Automatic Data Acquisition System monitored in a hybrid solar-electric dryer essential drying parameters in real time.
GERAR Mobile App made it possible to interconnect the user to the hybrid solar-electric dryer.
Automatic System is a viable option due to the facility of assembly as well as the open access Arduino platform.

ABSTRACT: Increasing the efficiency of solar dryers with ensuring that the system remains accessible to all users can be achieved with their automation through low-cost and easy-to-use technique sensors. The objective was to develop, implement and evaluate an automatic system for monitoring drying parameters in a hybrid solar-electric dryer (HSED). Initially, an automated data acquisition system for collecting the parameters of sample mass, air temperature, and relative air humidity was developed and installed. The automatic mass data acquisition system was calibrated in the hybrid solar-electric dryer. The automated system was validated by comparing it with conventional devices for measuring the parameters under study. The data obtained were subjected to analysis of variance, Tukey test and linear regression at p ≤ 0.05. The system to turn on/off the exhaust worked efficiently, helping to reduce the errors related to the mass measurement. The GERAR Mobile App showed easy to be used since it has intuitive icons and compatibility with the most used operating systems for mobile devices. The responses in communication via Bluetooth were fast. The use of Arduino, a low-cost microcontroller, to automate the monitoring activity allowed estimating the mass of the product and collecting the drying air temperature and relative air humidity data through the DHT22. This sensor showed a good correlation of mass and air temperature readings between the automatic and conventional system, but low correlation for relative air humidity. In general, the automatic data acquisition system monitored in real time the parameters for drying agricultural products in the HSED.

Key words: bluetooth, DHT22 sensor, Arduino, load cells

RESUMO: O aumento da eficiência de secadores solares com garantia de que o sistema permaneça acessível a todos os usuários pode ser alcançado com sua automação por meio de sensores de baixo custo e fácil utilização. Objetivou-se desenvolver, implantar e avaliar um sistema automático de monitoramento dos parâmetros de secagem em secador híbrido solar-elétrico (SHSE). Inicialmente, foi desenvolvido e instalado o sistema automático de aquisição de dados para a coleta dos parâmetros de massa da amostra e temperatura do ar e umidade relativa do ar de secagem. O sistema automatizado foi validado comparando-o com aparelhos convencionais de medição dos parâmetros em estudo. Os dados obtidos foram submetidos à análise de variância, teste de Tukey e regressão linear a p ≤ 0,05. O sistema ligar/desligar do exaustor funcionou de forma eficiente, reduzindo os erros relacionados à medição da massa. O GERAR Mobile App mostrou-se fácil de ser usado por possuir ícones intuitivos e compatibilidade com os sistemas operacionais mais utilizados para dispositivos móveis. As respostas na comunicação via Bluetooth foram rápidas. A utilização do Arduino, um microcontrolador de baixo custo, para automatizar a atividade de monitoramento permitiu estimar a massa do produto e coletar os dados de temperatura do ar de secagem e umidade relativa do ar por meio do DHT22. Este sensor mostrou boa correlação de leituras de massa e temperatura do ar entre o sistema automático e convencional, mas baixa correlação para umidade relativa do ar. Em geral, o sistema de aquisição de dados monitorou em tempo real os parâmetros para secagem de produtos agrícolas no SHSE.

Palavras-chave: bluetooth, sensor DHT22, Arduino, células de carga

• Ref. 252527 – Received 24 May, 2021
* Corresponding author - E-mail: juliana.lobop@yahoo.com.br
• Accepted 28 Oct, 2021 • Published 11 Nov, 2021
Editors: Josivanda Palmeiras Gomes & Carlos Alberto Vieira de Azevedo

Introduction

Several countries have started to concentrate efforts to expand the use of solar energy in various sectors to reduce the use of fossil fuels (Chen et al., 2019; Pelda et al., 2020; Lipińskia et al., 2021). In the agricultural sector, solar energy makes it possible to perform drying with a dryer that has low costs of installation and maintenance, in a clean way, with no risk of contaminating the environment and agricultural products (Kumar & Singh, 2020; Paes et al., 2020; Nukulwar & Tungikar, 2020). In order to improve the solar drying of agricultural products, it is necessary to invest in technology that use sustainable production processes associated with automation, seeking to follow the Industry 4.0 and Internet of Things (Wortmann & Flüchter, 2015; Enyoghasi & Badurdeen, 2021).

The collection of drying parameters is performed manually with interruptions throughout the process and in periods of the day of difficult execution. One way to overcome this problem may be automating the acquisition of data collected along the drying process (Goméz & Fernández, 2019). Automatic data acquisition systems have evolved considerably over the years, mainly due to technological advances in digital electronics and the introduction into the market of new low-cost and easily programmable electronic devices, such as Arduino boards (Dipova, 2017; Cid & Correa, 2019). The study of agricultural systems automation becomes a reality in the face of all technological development associated with the need for reliable and efficient systems to optimize the process. However, after a survey in the national and international literature, there was a scarcity in the study of collection of drying parameters through the automation of a solar dryer with Arduino, making it necessary for its dissemination throughout the scientific community.

The objective was to develop, implement and evaluate the automatic data acquisition system for continuously monitoring the parameters for drying agricultural products in the hybrid solar-electric dryer.

Material and Methods

The experiment was carried out in the hybrid solar-electric dryer (HSED) from the Institute of Technology, Engineering Department of the Universidade Federal Rural do Rio de Janeiro, on June 11 and 12, 2019. The mean air temperature and relative air humidity on these days were 26 °C and 75%, respectively.

The HSED comprises a solar collector, drying chamber, exhaust system and photovoltaic panel with a solar tracker, as described by Paes et al. (2020). A tray with dimensions of 0.54 m width and 0.44 m length was placed in the middle part of the drying chamber's interior. The tray is designed to hold nine removable baskets (0.14 m width, 0.10 m length, and 0.04 m height), equipped with a screen at the bottom, for the passage of drying air.

The experiment was carried out in three stages. The first was to develop and install the automatic data acquisition system (ADAS) for collecting the drying parameters of sample mass (m_{sample}, g) and drying air temperature (T, °C), and relative air humidity (RH, %). In the second stage, the load cells were calibrated in function of the standard mass and temperature inside the HSED. The third stage consisted of validating the ADAS through data collection of m_{sample}, T, and RH obtained with automatic monitoring (AM) and conventional monitoring (CM).

The ADAS was composed of an electronic panel, four load cells (measurement limits: ± 1000 g; operating T: - 40 to 80 °C; operating voltage: 3 to 12 V DC) to measure the variation of water mass in the sample and four DHT22 sensors (supply voltage: 3 to 5 V DC; operating range: - 40 to 80 °C ± 0.5% for T and 0 to 100% ± 2% for RH) to measure the drying air T and RH.

The Arduino Mega 2560 microcontroller (supply voltage: 6 to 20 V DC; 54 digital ports; 16 analog inputs; 256 KB Flash memory; 8 KB SRAM memory), HX711 amplifiers (operating T: -20 to 85 °C; operating voltage: 4.8 to 5.5 V DC; operating current: 1.6 mA) and Bluetooth BLE 4.0 modules (supply voltage: 3 to 5 V DC; range of 10 m; ISM 2.4 GHz.), relay module (supply voltage: 5 V DC; control voltage: 220 V AC; four channels) and RTC clock (operating T: - 40 to 85 °C; 56 bytes of SRAM) were connected to the electronic panel. Also, the serial connectors DB25 for the DHT22 sensors and DB15 for load cells were installed on the electronic panel to facilitate removal when necessary.

The electronic panel is placed inside an acrylic box installed on the side of the drying chamber and connected to it through a conduit. Inside the drying chamber, the cables were covered with a 2.5-mm-diameter heat-shrink tubing to avoid overheating, which could damage the insulation and cause short circuits (Figure 1).

Figure 1. Automated solar drying system: hybrid solar-electric dryer (A), drying chamber (B), acrylic box (C)

The load cells were installed on a metal structure fixed to the bottom of the four removable baskets. The metal structures were fixed in such a way that they kept the load cell in the central part of the removable basket. For each removable basket, a load cell was installed at positions P_1, P_2, P_3 and P_4 (Figure 2). Each load cell and metal structure assembly was fixed to a tray.

Two algorithms were developed to conduct the experiment, one for the acquisition, recording, and processing of data, performed using Arduino (Figure 3), and the other is the user interface via Bluetooth (Figure 4).

The communication between the user and the Arduino platform was made via Bluetooth. So, the GERAR Mobile App was created specifically for use in the HSED with the Inventor App, which is a visual, blocks language for building Android Apps.

The GERAR Mobile App layout was developed using intuitive icons to facilitate operations in the ADAS (Figure 5).

The AM by the ADAS was programmed to perform an average of 100 readings of the drying parameters in one hour, with the command to turn off the exhaust when reading the data, so that there is no interference in the reading. Data of

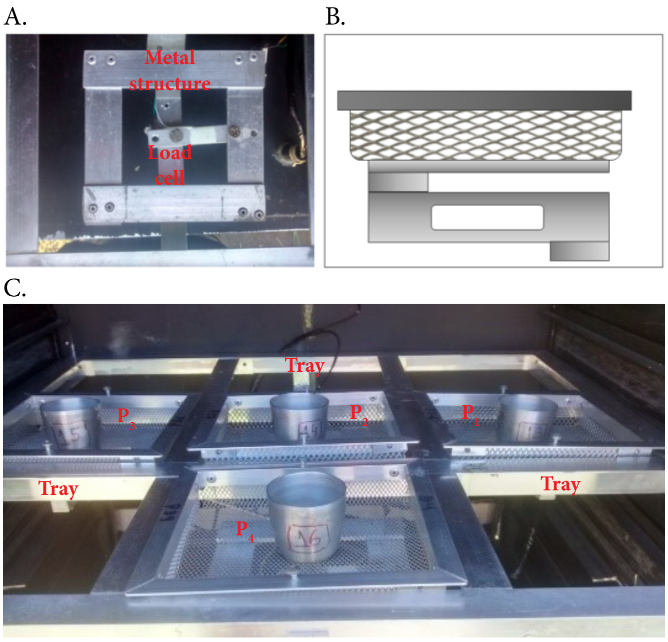

Figure 2. Load cell and metal structure assembly (A), basket on the assembly (B), baskets containing crucibles with samples on the tray (C)

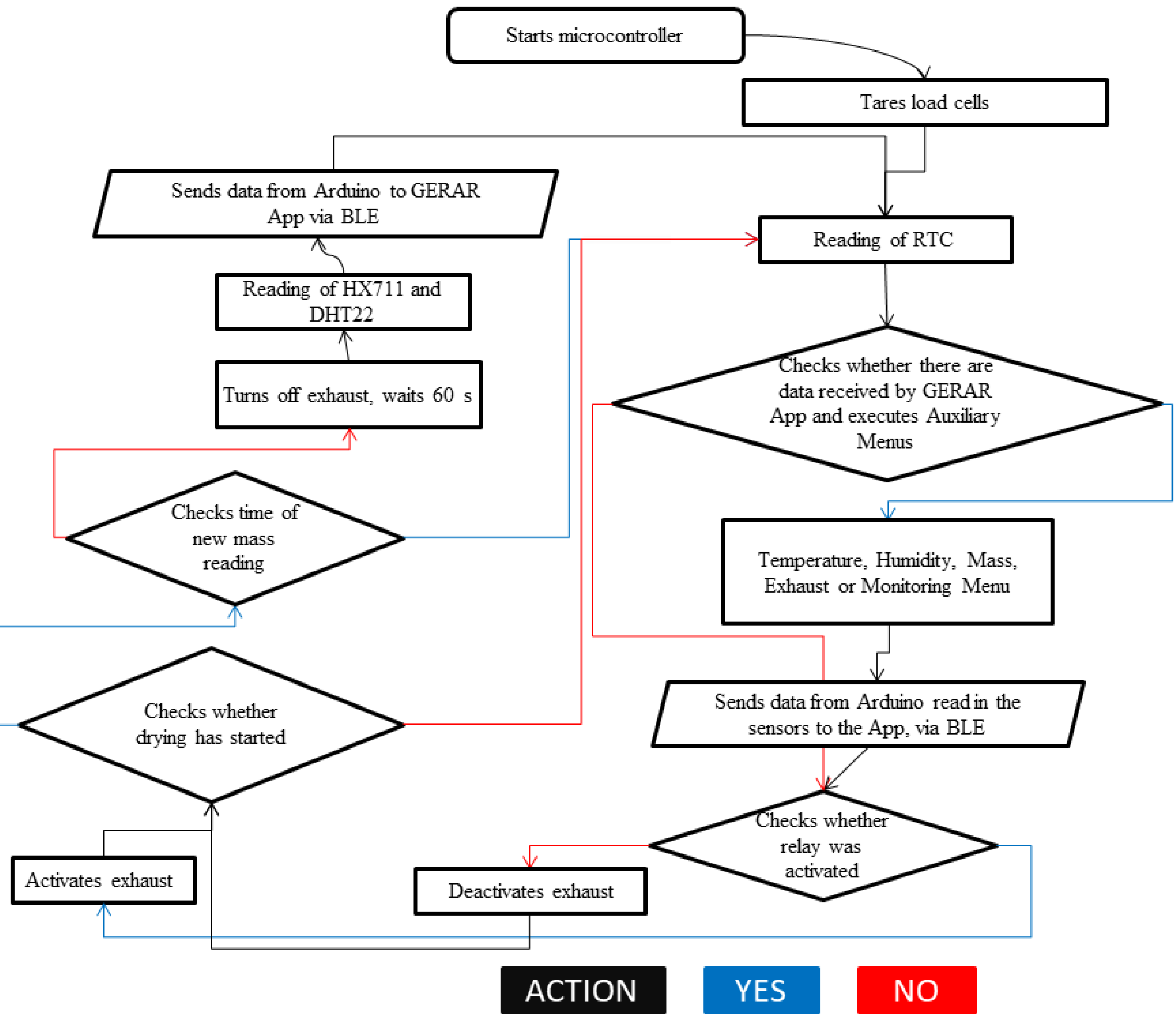

Figure 3. Flowchart of the algorithm developed on the Arduino platform

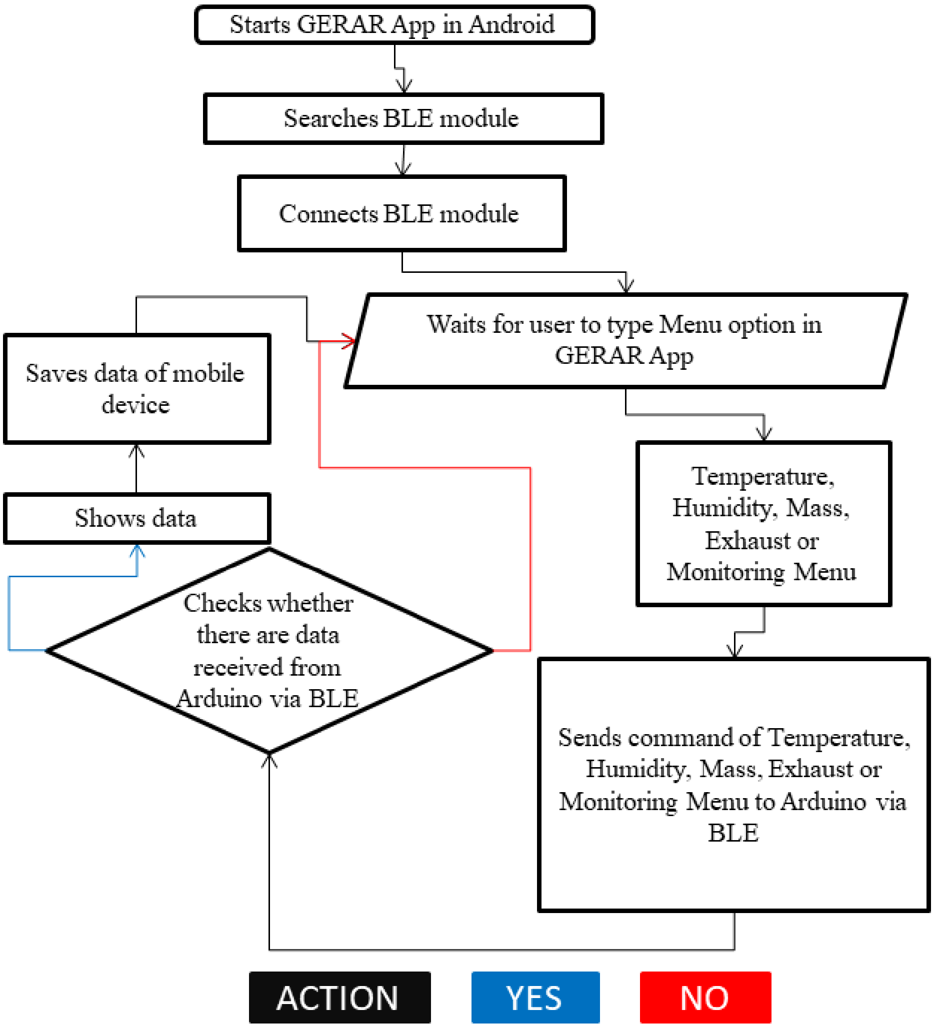

Figure 4. Flowchart for communication via Bluetooth

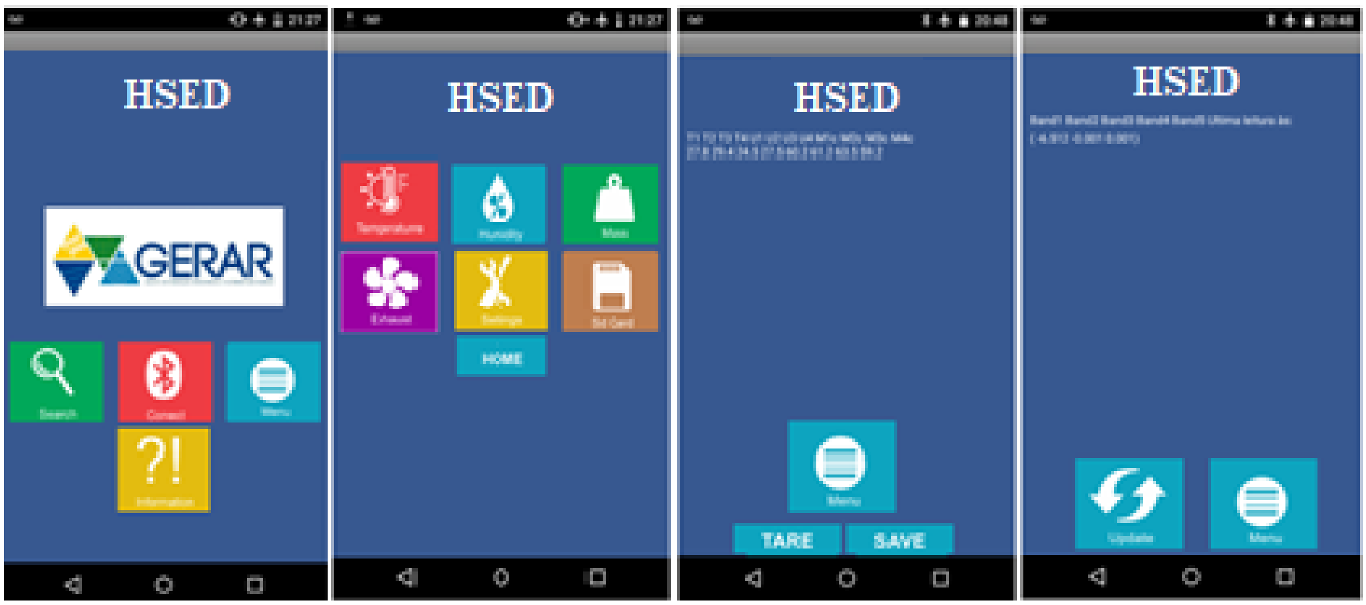

HSED - Hybrid solar-electric dryer

Figure 5. Application developed: Home screen (A), Menu screen (B), air temperature and relative air humidity monitoring screen (C), Sample mass monitoring screen (D)

m_{sample}, T and RH began to be collected by the ADAS 60 s after the exhaust was turned off.

The load cells were calibrated as a function of the operating temperature in the HSED in order to avoid possible sensor reading errors due to this parameter. The data collection temperature range inside the drying chamber was 25 to 50 °C with an interval of 5 °C. The operating temperature was kept constant due to a 127-V and 600-W ceramic conical resistance system installed at the base of the HSED drying chamber. The air temperature variation was controlled by an algorithm with an on/off system for the relay module. The on/off system was programmed in Arduino to maintain the air temperature in the drying chamber as defined by the user. The air temperature was monitored using a thermocouples connected to a millivoltmeter with the precision of ± 0.1 °C.

Calibration of load cells in the operating temperature range under study was performed with six standard masses from 50 to 300 g with 50 g intervals. The Arduino microcontroller connected to the HX711 amplifier collected data of the voltage variation caused in the load cell with the standard masses in the removable baskets. The reading of the standard masses was converted to a mass unit, in g, using the coefficient from the HX711 voltage amplifier's library.

The statistical analysis adopted in the calibration, consisted of calculating the relative error between the mass measured by the load cell and the standard mass of known mass (50, 100, 150, 200, 250 and 300 g) for each position (P_1, P_2, P_3 and P_4) and temperature (25, 30, 35, 40, 45 and 50 °C), totaling six replicates. In view of these results, the analysis of variance (ANOVA) by the F test at $p \leq 0.05$ was performed with the mean values of the relative error, adopting the factors position and temperature and interaction for each attribute. Then, the Tukey test at $p \leq 0.05$ was applied. The regression curves of the mean values of measured mass as a function of the standard mass for the temperature and position. Statistical analyses were performed with the statistical program Statistica, version 7.0 (StatSoft Inc. USA).

After calibrating the load cells with standard masses under different temperatures, data collection was started by AM by the ADAS and CM using conventional devices. The results of the drying parameters collected (m_{sample}, T and RH) in the HSED by the AM were compared with the values of CM. The conventional devices used were a precision bench scale model Marte, AD 500 (Sensitivity of 0.001 g), thermocouples connected to a millivoltmeter with the precision of ± 0.1 °C and thermo-hygrometer model MTH-1380. The drying air speed maintained at 1.0 m s^{-1} was monitored at the drying chamber's exhaust outlet using a digital thermo-anemometer model Minipa - MDA II.

In the CM, the data of drying parameters (m_{sample}, T and RH) and air speed were collected from 9:00 to 17:00 hours at 1 hour intervals, totaling 18 hours. However, the AM collected the data for 48 hours uninterruptedly, with records at one hour intervals. The data obtained by the AM at a different time from that of CM served to verify the continuous functioning of the automatic instrumentation.

For data collection to verify the loss of water from a given sample during the drying process, four aluminum crucibles containing inert material (sandy soil) and 10 mL of distilled water were used. The set (aluminum crucible, inert material and water) was dried in an oven at 105 °C for 24 hours. Each set was placed in the center of four different removable baskets in the tray located in the middle part of the drying chamber (Figure 2). The set was weighed on a precision scale periodically to determine the measured mass.

Data of air temperature and relative air humidity collection by thermocouples and thermo-hygrometer was performed close to the DHT22 sensors, distributed in four distinct points inside the HSED (exhaust outlet - S_1; tray - S_2; connection between drying chamber and solar collector - S_3; solar collector inlet - S_4).

The data obtained by AM of sample mass as a function of load cell position (P_1, P_2, P_3, and P_4) and air temperature and relative air humidity as a function of sensor position (S_1, S_2, S_3, and S_4) were compared to those collected with conventional devices in the CM. The results were analyzed using the ANOVA by the F test at $p \leq 0.05$. Statistical analyzes were performed with the statistical program Statistica, version 7.0 (StatSoft Inc. USA).

Results and Discussion

Concerning the algorithm developed, the system to activate/deactivate the exhaust worked efficiently, helping to reduce the errors related to the mass measurement. The GERAR Mobile App showed to be easy to use since it has intuitive icons and compatibility with the most used operating systems for mobile devices. The responses in communication via Bluetooth were fast. The signal range was 28.7 m, being considered satisfactory for the execution of the work, since there was no loss of connectivity, although the control panel was inside the acrylic protection. It is noteworthy that the data was stored in a folder on the cell phone.

The analysis of variance for the relative error between measured mass and standard mass indicates a significant effect at $p \leq 0.05$ by the F test for the variables position of the load cells (P), air temperature (T), and interaction between P and T (Table 1). Table 1 confirmed the need to calibrate the load cell for different temperatures, as each temperature required mass correction.

The relative error between the measured mass and the standard mass was higher in P_4, regardless of the T under study (Table 2). This effect was probably due to the proximity of P_4 to the drying chamber door (Figure 2). With this proximity, the act of opening and closing the door can cause instantaneous variations in the basket mass, as well as variation in $T_{drying\ air}$, due to the contact with ambient air.

A simple linear regression analysis between the measured mass and standard mass in the temperature range of 25 to 45 °C and 50 °C was done. Table 3 shows the equations generated in the linear regression analysis implemented in the Arduino algorithm. As each load cell has specific behavior, a single equation was not adopted. The R^2 values of the regression equations were very close to one, indicating a good fit of the data to the linear model. The R^2 values resulted from the comparison between the observed (measured mass) and estimated values generated by CM for the load cells calibration.

Table 1. Analysis of variance for relative error between measured mass and standard mass

Variable	DF	SS	MS	F	p-value
T	5	0.018248	0.003650	16.1262	0.000000
P	3	0.183334	0.061111	270.0229	0.000000
T × P	15	0.043967	0.002931	12.9515	0.000000
Error	120	0.027158	0.000226		

T - Air temperature; P - Position of the load cells; DF - Degrees of freedom; SS - Sum of squares; MS - Mean square

Table 2. Evaluation of the effect of air temperature and load cell position on the relative error between measured mass and standard mass

Load cell position	Temperature (°C)					
	25	30	35	40	45	50
P_1	0.00681 aB	0.00743 aB	0.002738 aB	0.005283 aB	0.00423 aB	0.01109 aB
P_2	0.00225 aB	0.00155 aB	0.000310 aB	0.000740 aB	0.00120 aB	0.00858 aB
P_3	0.00614 aB	0.00120 aB	0.009050 aB	0.002840 aB	0.00428 aB	0.01360 aB
P_4	0.09630 bA	0.05379 deA	0.088240 bcA	0.056010 cdA	0.06834 bcdA	0.17270 aA

See Figure 2 for load cell positions (P_1, P_2, P_3, P_4); Different uppercase letters in the same column represent significant differences in load cell position between the means subjected to Tukey test at $p \leq 0.05$; Different lowercase letters in the same row represent significant differences in air temperature between the means subjected to Tukey test at $p \leq 0.05$

Table 3. Regression equations fitted to measured mass and standard mass data and the respective coefficients of determination

Temperature (°C)	Load cell position	Equation	Coefficient of determination (R^2)	Standard error (g)
25-45	P_1	$y = 0.4311 + 1.0018^{**}x$	1.00	0.08
25-45	P_2	$y = 0.2811 + 1.0012^{**}x$	1.00	0.00
25-45	P_3	$y = 0.5137 + 1.0008^{**}x$	1.00	0.00
25-45	P_4	$y = -0.6580 + 0.9376^{**}x$	1.00	0.00
50	P_1	$y = -0.5034 + 0.9931^{**}x$	1.00	0.00
50	P_2	$y = 0.4921 + 1.0046^{**}x$	1.00	0.00
50	P_3	$y = 0.7780 + 1.0074^{**}x$	1.00	0.00
50	P_4	$y = -8.8713 + 0.9145^{**}x$	1.00	0.00
CV = 0.003%				

See Figure 2 for load cell positions (P_1, P_2, P_3, P_4); x - Mass measured in the load cell; y - Standard mass; ** - Significant at $p \leq 0.01$ by F test

The regression curves of the mean values of measured mass as a function of the standard mass showed a linear behavior, regardless of the load cell position and temperature under study (Figure 6). However, P_4 stands out from the other positions of the load cell both in the temperature range from 25 to 45 °C (Figure 6A) and at 50 °C (Figure 6B). The distinction of P_4 from the other load cell positions, being more pronounced at 50 °C, increases with the standard mass adopted, confirming the interference that occurs due to the proximity to the drying chamber door.

According to the ANOVA applied to the m_{sample} and $T_{drying\ air}$ data, AM and CM did not differ significantly in all positions of the load cell (P) and DHT22 sensor (S) installed in the HSED (Table 4). The mean $RH_{drying\ air}$ differed significantly between AM and CM for all sensor positions, except for S_4.

The m_{sample} reduced over the drying period in both AM and CM (Figure 7). However, in AM, the load cells located in P_4 (Figure 7D) showed irregular behavior. There was probably an error in the connections between the amplifier and the microcontroller. In the specific case of P_4, the proximity of the load cell to the drying chamber door may have aggravated the measurement error.

Table 4. Means of m_{sample}, T and RH of drying air collected by the automatic monitoring (AM) and conventional monitoring (CM)

Load cell position	Automatic monitoring	Conventional monitoring	p-value
Sample mass - m_{sample} (g)			
P_1	53.94	52.62	0.141224
P_2	54.25	52.59	0.120014
P_3	54.84	53.20	0.078577
P_4	51.26	52.51	0.457749
Drying air temperature - T (°C)			
S_1	34.35	34.65	0.833560
S_2	34.29	34.59	0.859281
S_3	34.62	34.84	0.899795
S_4	29.64	30.16	0.466446
Drying relative air humidity - RH (%)			
S_1	55.36	32.81	0.00033
S_2	55.12	17.90	0.00000
S_3	54.86	20.26	0.00000
S_4	60.55	59.54	0.71556

See Figure 2 for load cell positions (P_1, P_2, P_3, P_4); DHT22 sensor positions: exhaust outlet - S_1; tray - S_2; connection between drying chamber and solar collector - S_3; solar collector inlet - S_4; p - value of the F test

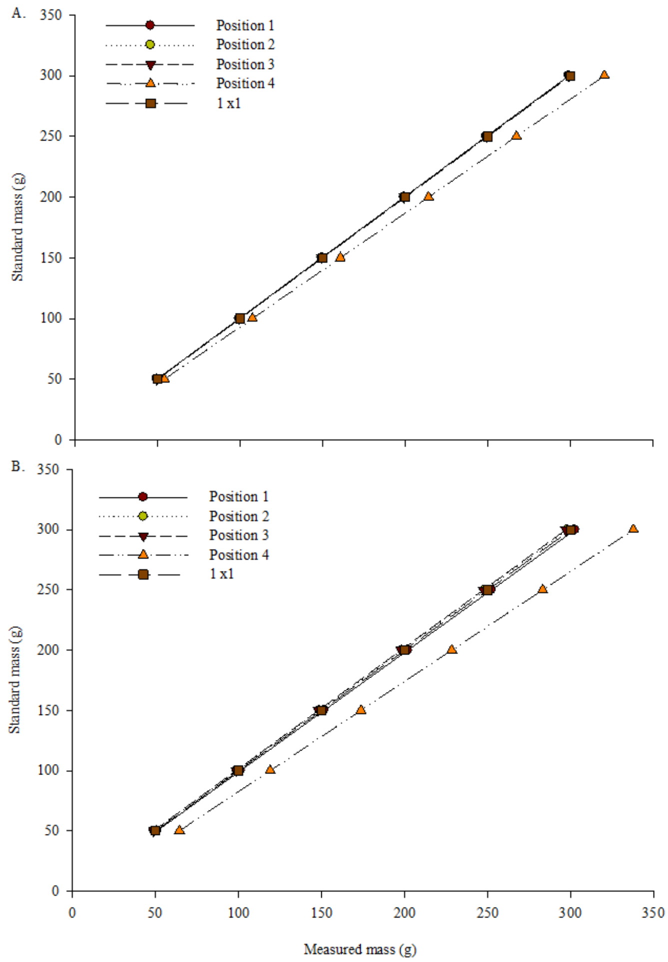

See Figure 2 for load cell positions (P_1, P_2, P_3, P_4)

Figure 6. Calibration curves of load cells to 25 to 45 °C (A), 50 °C (B)

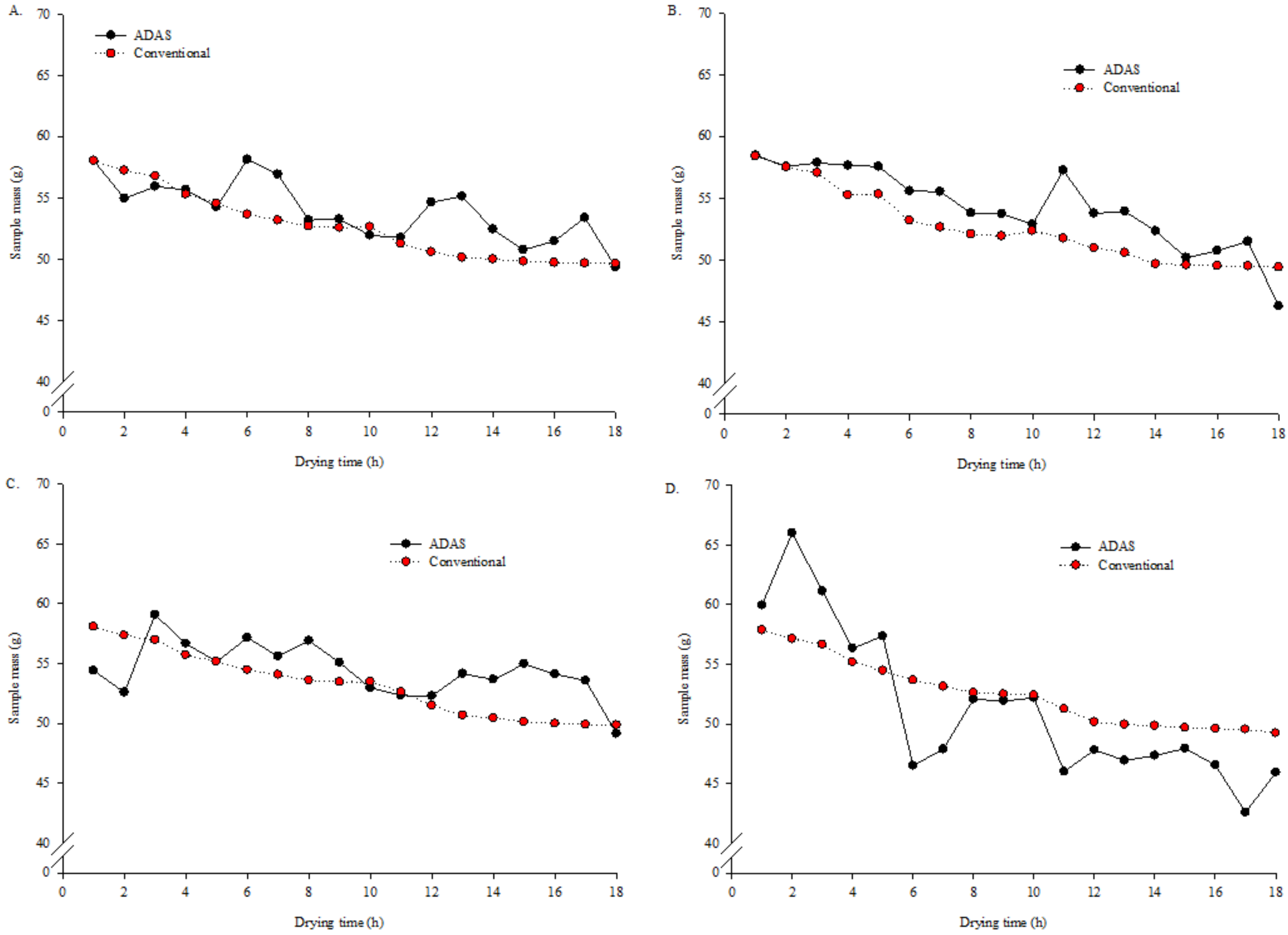

ADAS - Automatic data acquisition system; See Figure 2 for load cell positions (P_1, P_2, P_3, P_4)

Figure 7. Mass of samples as a function of drying time by automatic monitoring and conventional monitoring in P_1 (A), P_2 (B), P_3 (C) and P_4 (D)

Figure 8 shows that the values of $T_{drying\ air}$ measured by the AM (DHT22 sensor) were similar to those collected by CM (thermocouple connected to the millivoltmeter). Also, the variation of $T_{drying\ air}$ between 23.4 and 42.8 °C obtained by the DHT22 sensor indicates that data collection occurred within the sensor operating range. These results point to the system's reliability to increase the number of DHT22 sensors aiming at monitoring the drying air temperature in the HSED.

According to the Mali & Butale (2019), Kore et al. (2019), Patil et al. (2019a), and Patil et al. (2019b), implementing automation and design enhancement of the solar tunnel dryer with controlling circuit by Arduino UNO and temperature Sensor LM 35 accomplished the temperature control within the desired parameters and quality of agro products has been increased.

The standard behavior in the variation of $T_{drying\ air}$ values for the four data collection positions (S_1, S_2, S_3, and S_4) by

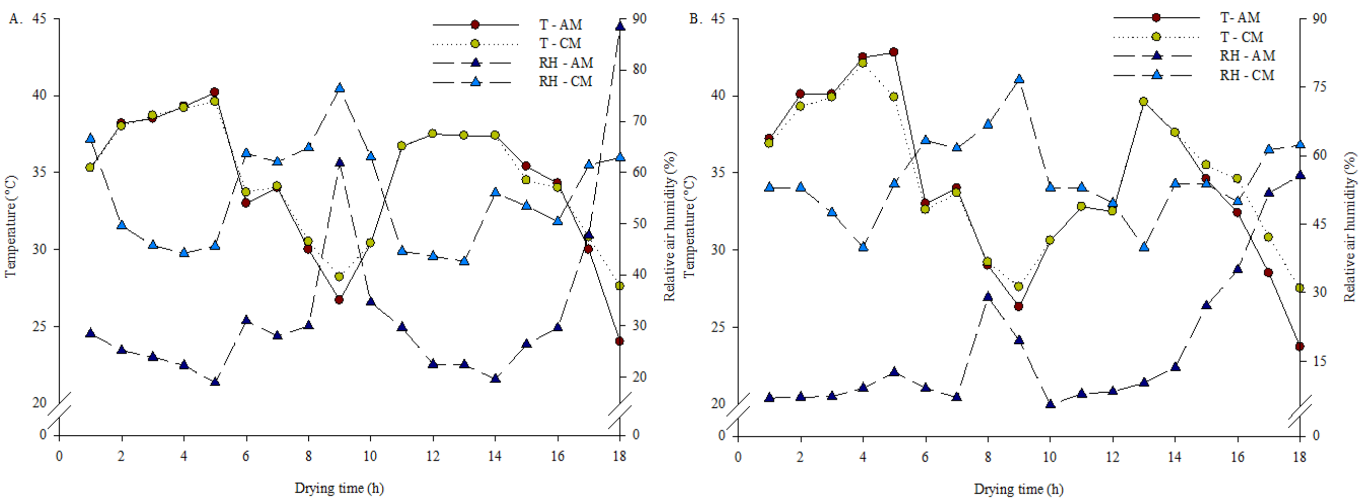

Continues on the next page

Continuation of Figure 8

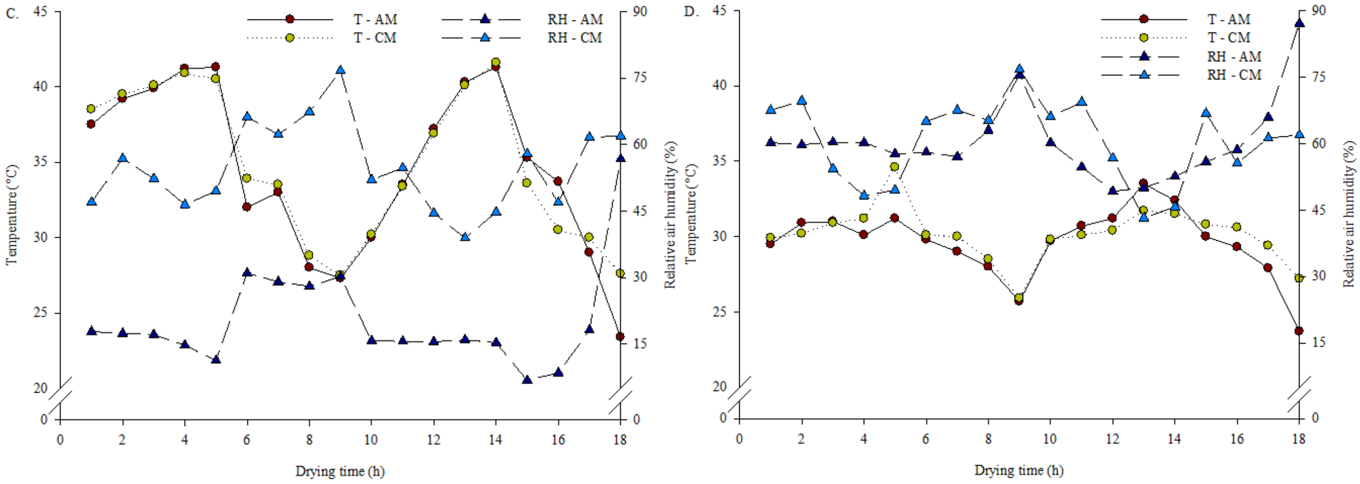

DHT22 sensor positions: exhaust outlet - S_1; tray - S_2; connection between drying chamber and solar collector - S_3; solar collector inlet - S_4

Figure 8. Drying air temperature (T) and relative air humidity (RH) as a function of drying time by automatic monitoring (AM) and conventional monitoring (CM) in the sensor positions S_1 (A), S_2 (B), S_3 (C), and S_4 (D)

AM (DHT22 sensor) and CM (thermo-hygrometer) was not verified for the $RH_{drying\ air}$. The $RH_{drying\ air}$ measured by the DHT22 sensor showed discrepant values compared to those collected by the thermo-hygrometer (Figure 8).

It can be observed that the behavior of $RH_{drying\ air}$ as a function of drying time obtained by AM and CM showed smaller differences only in S_4 - solar collector inlet (Figure 8D) compared to the other data collection positions. Thus, it can be inferred that DHT22 sensor does not have good accuracy and reliability to be used in drying processes aiming at the recording of $RH_{drying\ air}$. In the present study, the temperature range reached inside the drying chamber classifies the drying process as of low temperature (Jordan et al., 2020), which corroborates the hypothesis that DHT22 is not the ideal sensor for collecting RH data in drying processes. In this context, a strict and periodic remote monitoring of the parameters of mass loss, air temperature, and relative air humidity of drying becomes important. Inadequate conduction during the drying process results in losses of the agricultural product and excessive energy consumption, causing economic losses and generating environmental impacts.

As proposals to improve the ADAS, it is suggested to verify the effect of noise on load cells, automation of electrical resistances used in the drying process to supply temperature demand at night, construction of the printed circuit board to reduce errors in the connections and use of relative air humidity sensors with less error at high temperatures.

Conclusions

1. Automatic data acquisition system showed satisfactory results, since it monitored in real time parameters for drying agricultural products in hybrid solar-electric dryer.

2. However, it was necessary to take into account the position of data collection by the sensors, errors in the connections between the amplifier and the microcontroller.

3. Automated monitoring for measuring sample mass and air temperature showed compatible results with those of conventional monitoring, in all data collection positions.

4. Load cell positioning near the drying chamber door may affect the results.

5. The DHT22 sensor for relative air humidity measurement in the drying process was not reliable.

Literature Cited

Chen, W.; Yang, M.; Zhang, S.; Andrews-Speed, P.; Li, W. What accounts for the China-US difference in solar PV electricity output? An LMDI analysis. Journal of Cleaner Production, v.231, p.161-170, 2019. https://doi.org/10.1016/j.jclepro.2019.05.207

Cid, A. S.; Correa, T. V. Análise da variação de pressão em um tubo de Venturi utilizando Arduino e sensor de pressão. Revista Brasileira de Ensino de Física, v.41, p.1-7, 2019. https://doi.org/10.1590/1806-9126-rbef-2018-0333

Dipova, N. Design of low cost and innovative data acqusition in soil mechanics Testing using open source hardware. The Eurasia Proceedings of Science, Technology, Engineering & Mathematics, v.1, p.104-110, 2017.

Enyoghasi, C.; Badurdeen, F. Industry 4.0 for sustainable manufacturing: Opportunities at the product, process, and system levels. Resources, Conservation and Recycling, v.166, p.105362, 2021. https://doi.org/10.1016/j.resconrec.2020.105362

Goméz, B. E. C.; Fernández, J. A. P. Seguimiento remoto de variables ambientales en un secador solar, una apuesta IoT aplicada al agro. In: Quiroz, C. A. L. Sosteniblidad, cultura y sociedade. Medellín: IUPB, 2019. p.231-250.

Jordan, R. A.; Siqueira, V. C.; Cavalcanti-Mata, M. E. R. M.; Hoscher, R. H.; Mabasso, G. A.; Quequeto, W. D.; Battilani, M.; Freitas, R. L.; Oliveira, F. C. de; Martins, E. A. S. Sensorial quality of coffee submitted to dry at low temperature and cold with the use of a system based on heat pump technology. Research, Society and Development, [S. l.], v.9, p.1-18, 2020. https://doi.org/10.33448/rsd-v9i11.10302

Kore, S. S.; Patil, V. N.; Mane-Deshmukh, A. S.; Patil, D. R. Automatically controlled solar tunnel dryer using arduino for curry leaves. International Research Journal of Engineering and Technology, v.6, p.748-753, 2019.

Kumar, P.; Singh, D. Advanced technologies and performance investigations of solar dryers: A review. Renewable Energy Focus, v.35, p.148-158, 2020. https://doi.org/10.1016/j.ref.2020.10.003

Lipińskia, W.; Abbasi-Shavazi, E.; Chen, J.; Coventry, J.; Hangi, M.; Iyer, S.; Kumar, A.; Li, L.; Li, S.; Pye, J.; Torres, J. F.; Wang, B.; Wang, Y.; Wheeler, V. M. Progress in heat transfer research for high-temperature solar thermal applications. Applied Thermal Engineering, v.184, p.116-137, 2021. https://doi.org/10.1016/j.applthermaleng.2020.116137

Mali, M. S. B.; Butale, M. C. Automation of solar tunnel dryer using Arduino for sapota. International Research Journal of Engineering and Technology, v.6, p.1643-1649, 2019.

Nukulwar, M. R.; Tungikar, V. B. A review on performance evaluation of solar dryer and its material for drying agricultural products. Materials Today: Proceedings, v.46, p.345-349, 2020. https://doi.org/10.1016/j.matpr.2020.08.354

Paes, J. L.; Vargas, B. C.; Cunha, J. P. B.; Silva, D. S. C.; Ferraz, G. A. S.; Braz, M. R. S.; Ferraz, P. F. P.; Conti, L.; Rossi, G. Thermal performance of a solar hybrid dryer for Conilon coffee (*Coffea canephora*). Agronomy Research, v.18, p.2166-2184, 2020.

Patil, D. R.; Kore, S. S.; Patil, V. N.; Mane-Deshmukh, A. S.; Mali, S. B.; Durgade, D. P. Automatically controlled solar tunnel dryer using arduino for coriander. International Research Journal of Engineering and Technology, v.6, p.760-764, 2019a.

Patil, V. N.; Mane-Deshmukh, A. S.; Patil, D. R.; Kore, S. S. Automatically controlled solar tunnel dryer using arduino for potato. International Research Journal of Engineering and Technology, v.6, p.728-733, 2019b.

Pelda, J.; Stelter, F.; Holler, S. Potential of integrating industrial waste heat and solar thermal energy into district heating networks in Germany. Energy, v.203, p.1-10, 2020. https://doi.org/10.1016/j.energy.2020.117812

Wortmann, F.; Flüchter, K. Internet of things. Business & Information Systems Engineering, v.57, p.221-224, 2015. https://doi.org/10.1007/s12599-015-0383-3